JCTC Journal of Chemical Theory and Computation

Article

pubs.acs.org/JCTC

Benchmark Torsional Potentials of Building Blocks for Conjugated Materials: Bifuran, Bithiophene, and Biselenophene

Jacob W. G. Bloom and Steven E. Wheeler*

Department of Chemistry, Texas A&M University, College Station, Texas 77842, United States

Supporting Information

ABSTRACT: The utility of π-conjugated oligomers and polymers continues to grow, and oligofurans, oligothiophenes, and oligoselenophenes have shown great promise in the context of organic electronic materials. Vital to the performance of these materials is the maintenance of planarity along the conjugated backbone. Consequently, there has been a great deal of work modeling the torsional behavior of these prototypical components of conjugated organic materials both in the gas and condensed phases. Such simulations generally rely on classical molecular mechanics force fields or density functional theory (DFT) potentials. Unfortunately, there is a lack of benchmark quality, converged *ab initio* torsional potentials for bifuran, bithiophene, and biselenophene against which these lower level theoretical methods can be calibrated. To remedy this absence, we present highly accurate torsional potentials for these three molecules based on focal point analyses. These potentials will enable the benchmarking and parametrization of DFT functionals and classical molecular mechanics force fields. Here, we provide an initial assessment of the performance of common DFT functional and basis set combinations, to identify methods that provide robust descriptions of the torsional behavior of these prototypical building blocks for conjugated systems.

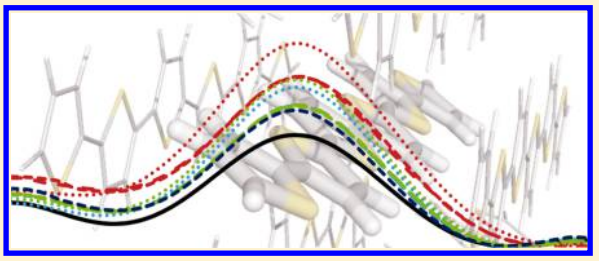

I. INTRODUCTION

Conjugated polymers and oligomers are vital for the development of next-generation organic electronic materials. Brédas et al. have reviewed the characteristics needed for effective organic semiconductors.[1,2] This includes a small band gap, which can be achieved through increased π-conjugation. Extended conjugation along the oligomer also promotes charge-transport along the chain. Consequently, planar and rigid oligomers are optimal.[3] In this context, there has been considerable computational and experimental work characterizing the torsional behavior of oligofurans, oligothiophenes, and oligoselenophenes. Among these conjugated systems, thiophene-based materials have seen the most widespread use. Furan and selenophene based materials, though less well-established, have been shown to have some properties that are more favorable than thiophene based oligomers.[4−6] In the case of oligofurans, these advantageous properties stem in part from their increased rigidity,[7] although oligoselenophenes and oligothiophenes have been shown to have comparable reorganization energies.[8]

In general, oligothiophenes, which are the most well established and extensively studied of the three systems in this study, do not exhibit a planar structure.[9−13] In fact, for bithiophene (Scheme 1), both the *syn* and *anti* planar configurations are transition states on the torsional potential. Many groups have attempted to devise planar thiophene based oligomers through the clever implementation of substituents or additional heteroatoms,[14] such as dialkoxybithiazole oligomers,[15] and Jackson et al. have provided a breakdown of the influence of various pairwise noncovalent interactions that can be exploited to enhance the planarity of these systems.[16]

Scheme 1. Structure of Bifuran (X = O), Bithiophene (X = S), and Biselenophene (X = Se)

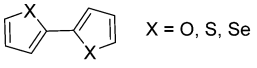

ϕ = X-C-C-X dihedral angle

The nonplanar geometry of bithiophene is well-established experimentally in both the gas and solution phases. Volden and co-workers determined the *syn* (ϕ = 35°) and *anti* (ϕ = 148°) conformations through electron diffraction.[17] Using LIF-excitation, hole-burning, and dispersed fluorescence spectroscopy, Takayanagi et al. confirmed the existence of a double-well potential (ϕ = 159° and 201°) around the *anti* conformation.[10] These symmetrically equivalent minima are separated by a barrier of about 25 cm^{-1} (0.07 kcal mol^{-1}). More recent work by Korter et al. using terahertz spectroscopy and several computational methods found that the torsional potential of bithiophene is similar in cyclohexane.[18] Although solution and gas phase torsional potentials are similar, with nonplanar minima, crystalline bithiophene exhibits a planar structure.[19,20] In particular, at 173 K, the crystal comprises about 15% planar *syn* conformer, while at 133 K, only the planar *anti* conformer is present. The planarity of bithiophene in the solid state has been attributed to crystal packing interactions,[3] and we previously

Received: March 17, 2014
Published: August 5, 2014

   dx.doi.org/10.1021/ct5004725 | *J. Chem. Theory Comput.* 2014, 10, 3647−3655

showed that the crystal environment leads to drastic changes in the torsional potential of oligothiophenes.[21]

Computational studies of the torsional potential of bithiophene have also been performed. For example, Raos et al. studied bithiophene using second-order Møller−Plesset perturbation theory (MP2) and coupled cluster theory [CCSD and CCSD(T)], finding a large spread in both the predicted torsional barrier heights and the dihedral angles of the *syn* and *anti* structures.[13] They noted that B3LYP and MP2 yield similar results when used with the aug-cc-pVTZ basis set. Fabiano and co-workers have also shown that various DFT functionals predict drastically different torsional potentials for bithiophene.[11]

Oligofurans have received much less attention, and unsubstituted oligofurans have only recently been created in lengths nearing double digits.[22] Moreover, previous computational studies have yielded varying results.[23−27] Sancho-García and Karpfen attempted to provide benchmark torsional potentials for bifuran.[28] They found that the MP2 energy is fairly well-converged with the cc-pVQZ basis set, and they reported a torsional potential based on MP2/cc-pVQZ energies appended with a CCSD(T)/cc-pVDZ correction. They also compared these data to a variety of DFT functionals with a cc-pVTZ basis set. They observe a shallow barrier to planarity for the *syn* conformer at every level of *ab initio* theory. Unfortunately, none of the functionals tested provide accurate barriers to planarity or torsional barriers.

Salzner and Aydin studied a range of DFT functionals for oligothiophenes and oligofurans, primarily with the 6-311G(d) basis set.[29] Comparing both geometric and electronic parameters with experimental data, they concluded that the most reliable functional for these systems is ωB97X-D.[29] However, the computed gas-phase structures were compared with experimental crystal structures, and it remains unclear whether ωB97X-D will perform well when compared to more reliable gas-phase computations.

To date, there have been limited studies of the torsional behavior of biselenophene and oligoselenophenes. In fact, the only experimental work on the torsional behavior of biselenophene is an NMR study of a nematic liquid crystal from 1979,[30] in which Veracini and co-workers reported a torsional angle of 22° for the *syn* conformer and 149° for the more prevalent *anti* conformation. Other work has focused on the characterization and production of new materials incorporating selenophenes.[31−33] Early computational work by Millefiori and Alparone, based on HF theory with small basis sets, confirmed the nonplanarity of both conformers of biselenophene in the gas phase.[34] More recent work from Elguero and co-workers applied B3LYP/6-311++G(d,p) and MP2/6-311++G(d,p) to a variety of systems, including bifuran, bithiophene, and biselenophene, finding similar energy minima.[35]

The parametrization of molecular mechanics potentials for conjugated oligomers has also been performed, as described in the recent review from Kohkhlov et al.[36] For example, Marcon and Raos expanded Allinger's MM3 force field to include explicit parametrization for the inter-ring bithiophene torsional potential based on MP2/aug-cc-pVTZ.[37] Ultimately, they showed that these force fields reproduce crystal structure geometries of polythiophenes. More recent work by Friesner et al. reparameterized the OPLS potential based on a bithiophene potential computed using LMP2.[38] Similarly, Jorgensen and co-workers[39] parametrized and tested the OPLS all-atom force field for a series of biaryl systems based on MP2 benchmarks. Overall, it is advantageous to parametrize and assess the performance of MM potentials against MP2 and higher-level torsional potentials for small model systems to ensure the accuracy of calculations of larger oligomers.[6,29,40]

Brédas and co-workers[41] very recently presented a detailed study of torsional potentials for polyacetylene and polydiacetylene. Ultimately, they showed[41] that predicted torsional barrier heights are sensitive to both percent exact exchange as well as the value of the range-separation parameter used in long-range corrected DFT functionals. Here, we report high-accuracy torsional potentials for bithiophene, bifuran, and biselenophene and then provide a preliminary assessment of the performance of popular DFT functionals and basis set combinations. The identification of DFT functionals that provide an accurate description of the torsional potentials of these simple model systems should open the door for rigorous studies of the torsional behavior of larger oligofurans, oligothiophenes, and oligoselenophenes.

II. THEORETICAL METHODS

Torsional potentials for bifuran, bithiophene, and biselenophene were determined by constraining the X−C−C−X dihedral angle (X = O, S, and Se) at 5° intervals from 0° to 180° and optimizing all other internal coordinates. The energy and dihedral angle for the stationary points along these potentials were interpolated from these scans through a quadratic fit to nearby points. Benchmark torsional potentials were derived using focal point analyses (FPA),[42−44] in which one executes dual expansions of the one- and *N*-particle basis sets at a fixed optimized geometry. The extrapolation of a series of valence electronic energies enable the systematic approach to the complete basis set Born−Oppenheimer result. Details of the procedure have been described previously.[45] For these FPA computations, energies were executed at geometries optimized using MP2 paired with the aug-cc-pVTZ basis set. MP2 and Hartree−Fock (HF) energies were computed with the correlation consistent cc-pVXZ basis sets (X = D, T, Q, and 5), while CCSD and CCSD(T) energies were computed with cc-pVXZ (X = D, T, and Q).[46−48] HF energies were extrapolated using an exponential form[49] based on energies computed with the cc-pVXZ basis sets (X = T, Q, and 5), while correlation energies were extrapolated separately using the functional form of Helgaker et al.[50] using cc-pVTZ and cc-pVQZ energies. Coupled-cluster and MP2 energies were evaluated using Molpro.[51] Additional single point energies at the CCSDT/cc-pVDZ level were carried out using CFOUR[52] for the fully planar geometries (ϕ = 0° and 180°), to gauge the convergence of the predicted torsional energies toward the FCI limit. Core electrons were frozen in all correlated computations.

At many torsional angles, the Hartree−Fock wave functions for these systems exhibit spin-instabilities, suggesting potentially significant diradical character. However, examination of the T-amplitudes of the coupled cluster wave functions does not indicate any significant multireference character (T_2 amplitudes are listed in Supporting Information, Tables S9−S11), and CCSD(T) computations based on nonsymmetry-broken HF reference wave functions should provide reliable energies. This is corroborated by the rapid convergence of the coupled cluster energies toward the FCI limit for these systems (*vide infra*).

We assessed the performance of 12 popular DFT functionals (B2PLYP,[53] B2PLYP-D,[54] B3LYP,[55−58] B3LYP-D,[55−59] B97-

Table 1. Incremental Focal Point Analyses (kcal mol^{-1}) of the Energy Difference between Planar *syn* and *anti* Conformers of Bifuran, Bithiophene, and Biselenophene[a]

	HF	+δ(MP2)	+δ(CCSD)	+δ[CCSD(T)]	+δ(CCSDT)	=CCSDT
			Bifuran			
cc-pVDZ	2.62	−0.81	+0.36	−0.07	−0.01	2.09
cc-pVTZ	2.31	−0.77	+0.35	−0.11	[−0.01]	[1.78]
cc-pVQZ	2.30	−0.81	+0.38	−0.12	[−0.01]	[1.74]
cc-pV5Z	2.31	−0.85	[+0.41]	[−0.12]	[−0.01]	[1.74]
CBS limit	[+2.32]	[−0.89]	[+0.44]	[−0.13]	[−0.01]	[1.74]
			Bithiophene			
cc-pVDZ	1.33	−0.48	+0.23	−0.08	+0.01	1.01
cc-pVTZ	1.28	−0.61	+0.31	−0.11	[+0.01]	[0.87]
cc-pVQZ	1.25	−0.66	+0.33	−0.13	[+0.01]	[0.81]
cc-pV5Z	1.23	−0.68	[+0.34]	[−0.13]	[+0.01]	[0.77]
CBS limit	[+1.22]	[−0.70]	[+0.36]	[−0.14]	[+0.01]	[0.75]
			Biselenophene			
cc-pVDZ	1.89	−0.60	+0.27	−0.09	+0.00	1.48
cc-pVTZ	1.92	−0.77	+0.37	−0.14	[+0.00]	[1.38]
cc-pVQZ	1.91	−0.83	+0.39	−0.15	[+0.00]	[1.31]
cc-pV5Z	1.91	−0.87	[+0.40]	[−0.16]	[+0.00]	[1.29]
CBS limit	[+1.90]	[−0.90]	[+0.42]	[−0.17]	[+0.00]	[1.26]

[a]Numbers in parentheses represent extrapolated values, except for the CCSDT column, in which additivity is assumed.

D,[59,60] M06,[61] M06-2X,[61] M06-HF,[61] PBE,[62,63] PW91,[64−66] ωB97X,[67] and ωB97X-D[68]) in order to pinpoint functionals that provide robust descriptions of the torsional behavior of these three model systems. These functionals span the gamut of modern DFT approximations, including GGAs (PBE, PW91, and B97-D), hybrid GGAs (B3LYP), hybrid meta-GGAs (M06, M06-2X, M06-HF), double-hybrid GGAs (B2PLYP and B2PLYP-D), and range-corrected functionals (ωB97X and ωB97X-D). Each of these functionals was tested with six representative basis sets [6-31+G(d), 6-31++G(d),[69−73] 6-311++G(d),[71,73−75] cc-pVDZ,[46−48,76] aug-cc-pVTZ,[46−48,76,77] and def2-TZVPP[78−80]] The 6-31G, 6-31++G, 6-31G(d), 6-31G(d,p), 6-31+G(d,p), and 6-31++G(d,p) basis sets were also considered with the B97-D functional, to explore the impact of various combinations of diffuse and polarization functions. The M06-2X functional is known to be particularly sensitive to DFT integration grids.[81−84] As such, we have used an extra-fine integration grid with 99 radial and 590 angular points for the M06-2X computations. All DFT computations were executed using Gaussian09.[85]

The performance of double-ζ Pople-style basis sets was assessed (relative to the FPA benchmarks, see below) using the B97-D functional to quantify the impact of diffuse and polarization functions on predicted torsional potentials for bifuran, bithiophene, and biselenophene. This functional was chosen primarily because it exhibits the greatest deviations from the FPA benchmarks (*vide infra*), so it has more room for improvement through changes in basis set. However, it is assumed that the basis set dependence of all of the tested functionals will be similar, and these results are representative of the larger set of functionals considered below. Computed torsional potentials are provided in Figure S1 in the Supporting Information. For bifuran, the inclusion of either diffuse or polarization functions provides little improvement; similarly, 6-311++G(d) offers negligible improvement over these double-ζ basis sets.

In contrast, the torsional potentials for bithiophene are much more sensitive to changes in basis set. In particular, for the double-ζ Pople-style basis sets, polarization functions on the heavy atoms are more important than diffuse functions. In fact, without polarization functions, B97-D predicts a nearly planar geometry for the *anti* conformer of bithiophene. The B97-D predicted barrier is more reliable upon inclusion of diffuse functions on the heavy atoms, regardless of whether polarization functions are included. The best results are provided when both polarization and diffuse functions are included for the heavy atoms. On the other hand, the inclusion of diffuse or polarization functions on the hydrogen atoms does not provide appreciable improvement in the predicted potentials. Similarly, 6-311++G(d) does not provide significantly more accurate potentials than 6-31+G(d).

Comparison of Pople-style basis sets for biselenophene is more problematic, because several definitions exist for the 6-31G family of basis sets for selenium.[86−90] Here, we considered two of these definitions: 1) the earlier, pseudo-6-31G basis set of Binning and Curtiss[88] (BC6-31G), which contains the Dunning correlation consistent primitives, and 2) the 6-31G basis set based on the prescription introduced by Rassolov et al.[89] (6-31G). Additionally, we found no optimized diffuse functions parametrized for selenium and either the 6-31G or 6-311G basis sets. Consequently, the 6-31+G, 6-31+G(d), and 6-31+G(d,p) basis sets for Se included diffuse functions from the aug-cc-pVDZ basis set.[23d,25]

For biselenophene, the BC6-31G basis set of Binning and Curtis[88] tends to provide unphysical, disfigured potentials if diffuse functions are included (see SI Figure S2). Moreover, for many points along these torsional potentials, this basis set lead to severe SCF convergence problems. Oddly, in the absence of diffuse functions, this 6-31G basis set provides potentials with a qualitatively correct shape but with a transition state that is much too high. Islam et al. reported similar issues with the BC6-31G basis sets for a range of third row atoms.[91,92] The newer 6-31G basis sets for selenium, from Rossalov et al.,[42] provide marked improvement; for this reason, we use the newer definition below. For biselenophene, the inclusion of polarization functions on the heavy atoms provides a slight improvement to the potential, while diffuse functions on the heavy atoms have a more profound effect. However, in contrast

to the behavior for bifuran and bithiophene, for biselenophene the 6-311++G(d) basis set provides considerably more reliable potentials (when paired with B97-D) than any of the Pople-style double-ζ basis sets and is recommended for applications to oligoselenophenes.

III. RESULTS AND DISCUSSION

The torsional potentials for bifuran, bithiophene, and biselenophene have been thoroughly studied. First, features of the FPA-derived potentials are discussed, and the performance of *ab initio* methods assessed. This is followed by a broader assessment of the performance of popular DFT functional and basis set combinations for the torsional potentials of these model conjugated systems.

A. Benchmark Torsional Potentials. Focal point analyses were executed at MP2/aug-cc-pVTZ optimized geometries for each point along the torsional potentials of bifuran, bithiophene, and biselenophene. Incremental focal point data are listed in Table 1 for the energy difference between planar *syn* and *anti* bifuran, bithiophene, and biselenophene. These data show rapid convergence with respect to both basis set and inclusion of electron correlation effects. In particular, the CCSD(T)/cc-pVQZ energies are within 0.05 kcal mol^{-1} of the complete basis set (CBS) limit. Similarly, the full treatment of triple excitations provides only modest corrections to the CCSD(T) values. Consequently, the effects of triple excitations are well-approximated at the CCSD(T) level, and iterative treatment of triple excitations should not be necessary for other points along these torsional potentials. Moreover, the spin-symmetry breaking that plagues the HF wave functions for these systems does not appear to significantly hamper the convergence of the coupled cluster expansion built on a nonsymmetry-broken reference.

Based on these points, the FPA energies for each point along the torsional potentials should be converged to well within 0.1 kcal mol^{-1} of the *ab initio* limit. In fact, both CCSD(T)/cc-pVQZ and MP2/cc-pVQZ provide potentials closely approach the benchmark FPA data (see Figure 1); for smaller basis sets there are much more substantial deviations. The agreement between MP2/cc-pVQZ and the benchmark curves is likely due to error cancellation, as the CCSD/cc-pVQZ potential differs more substantially from the FPA result. Additionally, the MP2/cc-pVQZ potential for bifuran underestimates the overall curvature. Regardless, the present results suggest that MP2, if paired with a sufficiently large basis set, should provide near quantitative predictions of the torsional potentials of bifuran, bithiophene, and biselenophene. Thus, the popular use of MP2 in the parametrization of MM force fields is justified,[36−39] assuming that sufficiently large basis sets are used.

Characteristics of the stationary points on the FPA torsional potentials are listed in Table 2. In each of the systems, there is a negligible barrier to planarity for both the *syn* and *anti* minima, and the *syn-anti* torsional barriers range from only 2.2 kcal mol^{-1} (for biselenophene) to 4.0 kcal mol^{-1} (bifuran). The data for both bifuran and bithiophene agree with previous studies. For example, for bithiophene, the *syn* minimum is planar and is higher-laying than the minimum associated with the *anti* conformer, as seen experimentally.[19,20] Moreover, the FPA-predicted torsional angle for the *syn* and *anti* conformers of bithiophene (35.4° and 158.9°) agree with the experimentally derived torsional minima (35° and 148°).[17] Finally, we note that the FPA-predicted barrier to planarity for the *anti* conformer of bithiophene (0.12 kcal mol^{-1} = 42 cm^{-1}) is in reasonable agreement with the experimental value of 25 cm^{-1}.[10] As also demonstrated by Sancho-García and Karpfen,[28] the *syn* side of the bifuran potential exhibits a very shallow nonplanar energy minimum at ϕ = 16°. This stationary point is 0.03 kcal mol^{-1} lower than the planar structure and most likely has no discernible effect on the molecule; however, it does indicate that the same effects causing nonplanarity in bithiophene are at play in bifuran but to a much lesser degree. The presence of a similar minimum on the *anti* side is not evident in this 5° scan; however, a finer scan may indicate a very small nonplanar minimum.

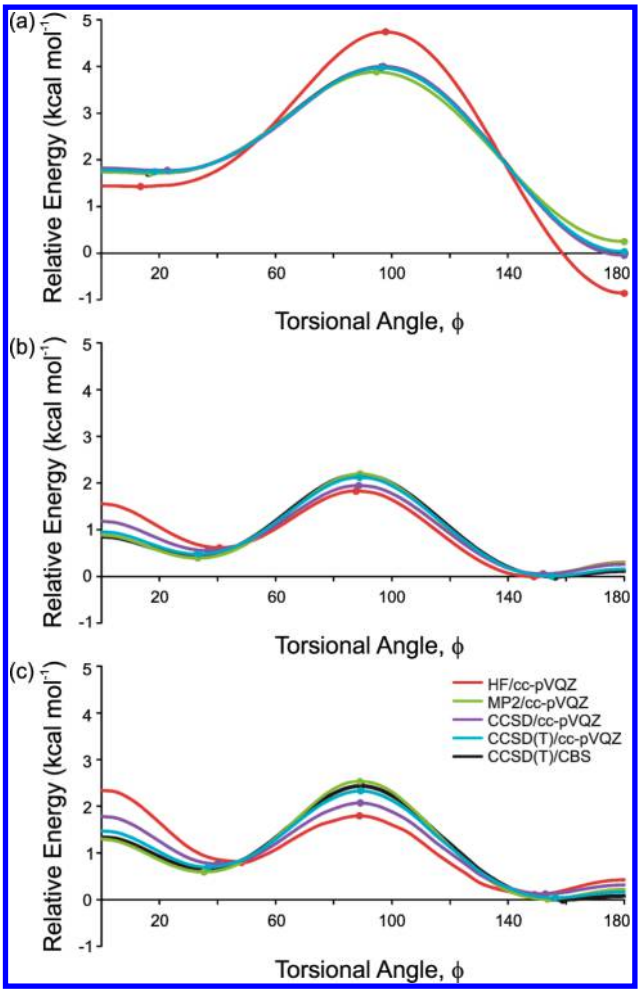

Figure 1. Torsional potential energy curves for (a) bifuran, (b) bithiophene, and (c) biselenophene at various levels of *ab initio* theory. The dots indicate the interpolated position of the stationary points along these curves.

These torsional potentials reveal important differences and similarities among bifuran, bithiophene, and biselenophene. First, bifuran has essentially planar minima for both the *syn* and *anti* conformations, while bithiophene and biselenophene do not. Also, the depth of the double-well potential for the *anti* conformer of bithiophene is nearly twice that of biselenophene, although in both cases the barrier to planarity is comparable with k_BT at ambient temperatures. Perhaps more importantly, the potential energy curve for bifuran surrounding the *anti* conformation is much narrower than for either bithiophene or biselenophene. For example, at 0.5 kcal mol^{-1}, the bifuran energy well spans angles deviating from the planar *anti* geometry by 20°, while for bithiophene and biselenophene

dx.doi.org/10.1021/ct5004725 | J. Chem. Theory Comput. 2014, 10, 3647−3655

Table 2. Relative Energies (E, in kcal mol^{-1}) and Torsional Angles (ϕ, in deg) for Stationary Points along Torsional Potentials of Bifuran, Bithiophene, and Biselenophene Based on Benchmark FPA Potentials

	anti		TS		*syn*		barrier to planarity	
	E	ϕ	E	ϕ	*E*	ϕ	*anti*	*syn*
bifuran	0.00	180.0	3.99	96.5	1.72	16.3	0.00	0.03
bithiophene	0.00	156.3	2.18	89.0	0.44	32.3	0.12	0.42
biselenophene	0.00	158.9	2.43	89.4	0.65	35.4	0.08	0.69

the points 0.5 kcal mol^{-1} above the *anti* minima are 50° from planarity. These differences underscore the torsional flexiblility of oligothiophenes and oligoselenophenes and the relative rigidity of oligofurans.

B. Functional and Basis Set Performance. The performance of DFT functionals and basis sets, when compared to the benchmark potentials, were analyzed based on their ability to reproduce the relative energy of the *syn* and *anti* minima, as well as the torsional barriers for bifuran, bithiophene, and biselenophene. DFT-predicted torsional potentials for selected functionals are shown in Figure 2, along with the benchmark FPA potentials. With regard to the relative energy and dihedral angles of the *syn* and *anti* minima, when compared to the benchmark FPA data, the DFT functionals tested perform remarkably well. Indeed, the maximum error in the predicted energy difference between the *syn* and *anti* conformers is only 0.39 kcal mol^{-1}. Errors in predicted energies are provided in Table 3. Errors in predicted dihedral angles are available in SI Tables S1 and S2. Intriguingly, empirical dispersion corrections provide little, if any, improvement in predicted conformational energies. Indeed, B2PLY-D, B3LYP-D, and ωB97X-D all exhibit errors consistently larger than those of their non-dispersion-corrected counterparts. The impact of the amount of exact exchange is less straightforward. In particular, for bifuran and biselenophene, M06-2X (with 54% HF exchange) provides the most accurate relative conformational energies, whereas M06-HF (100% HF exchange) is more accurate for bithiophene.

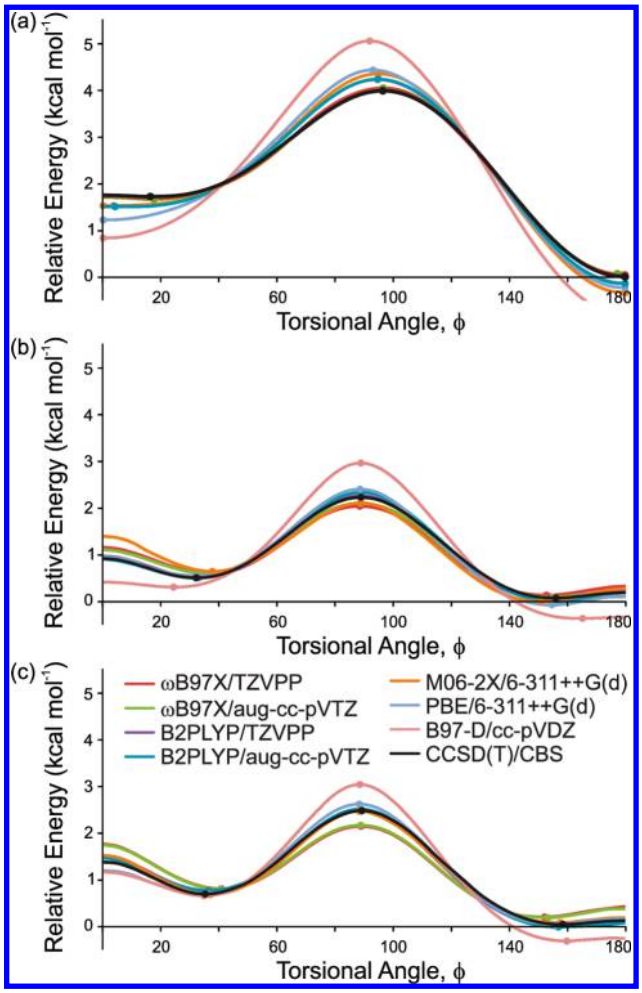

Figure 2. Benchmark CCSD(T)/CBS potential energy curve for (a) bifuran, (b) bithiophene, and (c) biselenophene, along with potential energy curves from selected DFT methods and basis sets. The dots indicate the interpolated position of the stationary points along these curves. These curves are shifted to minimize the RMS deviation from the reference CCSD(T) potential.

For bifuran, the best performing combination of functional and basis set is ωB97X paired with 6-31+G(d) or 6-31++G(d). These levels of theory accurately predict the energy separation between the *syn* and *anti* conformers as well as the dihedral angle of the *syn* conformer. Intriguingly, ωB97X predicts a slightly twisted geometry for the *anti* conformer. On the whole, five functional/basis set combinations (four with ωB97X-D and one with ωB97X) predicted *anti* conformers that deviate from planarity. However, given the flat nature of the potential in this region, this twisting should have a negligible impact on performance. The pure DFT functional B97-D, when paired with cc-pVDZ, predicts the relative energy of the *syn* conformer to within 0.05 kcal mol^{-1} of the FPA benchmark; however, this level of theory fails to capture the nonplanarity of the *syn* conformer of bifuran. Indeed, very few of the functionals are able to capture the existence of the gauche *syn* conformer, with most levels of theory tested predicting a planar geometry for the *syn* conformer. Overall, the Pople-style basis sets tend to provide more accurate torsional potentials for bifuran than either the Dunning or Ahlrichs basis sets.

For bithiophene, a number of functional and basis set combinations provide conformational energies energies that deviate from the FPA data by less than 0.1 kcal mol^{-1}. However, unlike the bifuran case, B97-D is the worst performing functional for bithiophene, although the mean error across all basis sets is still only 0.21 kcal mol^{-1}. On the other hand, B2PLYP, ωB97X, and ωB97X-D all provide very reliable conformational energies for bithiophene. In general, the Pople-style basis sets do not fare as well, and the Ahlrichs TZVPP basis tends to lead to the most accurate torsional potentials. However, M06-HF provides the most robust performance for this system, with errors less than 0.1 kcal mol^{-1} regardless of the basis set employed.

The most accurate torsional potentials for biselenophene are provided by B2PLYP-D/6-31+G(d) and PW91/6-311++G(d), which predict energies for the *syn* conformer in essentially exact agreement with the FPA value. Moreover, the predicted dihedral angles for the *syn* and *anti* minima are both within 1° of the benchmark values. However, B3LYP and M06-2X are

Table 3. Errors in Predicted Energies (kcal mol^{-1}) for the *syn* Conformer, Relative to the *anti* Conformer, When Compared to the FPA Values

	6-31+G(d)	6-31++G(d)	6-311++G(d)	cc-pVDZ	aug-cc-pVTZ	TZVPP	**mean**
			Bifuran				
B2PLYP	0.02	0.03	0.02	0.33	0.06	0.05	**0.09**
B2PLYP-D	0.07	0.07	0.07	0.36	0.02	0.01	**0.10**
B3LYP	0.05	0.06	0.10	0.35	0.09	0.06	**0.12**
B3LYP-D	0.11	0.12	0.15	0.41	0.03	0.00	**0.14**
B97-D	0.14	0.15	0.15	0.05	0.25	0.22	**0.16**
M06	0.15	0.16	0.11	0.40	0.10	0.11	**0.17**
M06-2X	0.03	0.05	0.15	0.32	0.04	0.00	**0.10**
M06-HF	0.26	0.27	0.39	0.51	0.24	0.19	**0.31**
PBE	0.28	0.28	0.26	0.14	0.36	0.33	**0.28**
PW91	0.23	0.23	0.22	0.12	0.33	0.30	**0.24**
ωB97X	0.01	0.01	0.04	0.23	0.12	0.08	**0.08**
ωB97X-D	0.08	0.05	0.03	0.21	0.20	0.17	**0.12**
mean	**0.12**	**0.12**	**0.14**	**0.29**	**0.15**	**0.13**	**0.16**
			Bithiophene				
B2PLYP	0.05	0.08	0.15	0.12	0.07	0.03	**0.08**
B2PLYP-D	0.11	0.14	0.21	0.19	0.14	0.10	**0.15**
B3LYP	0.20	0.20	0.22	0.19	0.12	0.08	**0.17**
B3LYP-D	0.29	0.30	0.32	0.31	0.24	0.18	**0.27**
B97-D	0.24	0.25	0.26	0.24	0.17	0.13	**0.21**
M06	0.23	0.27	0.29	0.18	0.17	0.13	**0.21**
M06-2X	0.14	0.15	0.21	0.11	0.13	0.07	**0.13**
M06-HF	0.04	0.03	0.08	0.02	0.03	0.01	**0.04**
PBE	0.17	0.19	0.19	0.13	0.07	0.02	**0.13**
PW91	0.18	0.19	0.20	0.14	0.08	0.03	**0.14**
ωB97X	0.08	0.08	0.14	0.09	0.06	0.02	**0.08**
ωB97X-D	0.02	0.03	0.08	0.01	0.03	0.06	**0.04**
mean	**0.15**	**0.16**	**0.20**	**0.14**	**0.11**	**0.07**	**0.14**
			Biselenophene				
B2PLYP	0.18	0.12	0.13	0.08	0.12	0.10	**0.12**
B2PLYP-D	0.00	0.05	0.02	0.17	0.24	0.21	**0.11**
B3LYP	0.01	0.05	0.01	0.15	0.18	0.17	**0.09**
B3LYP-D	0.29	0.32	0.20	0.32	0.35	0.35	**0.31**
B97-D	0.24	0.28	0.17	0.32	0.31	0.32	**0.27**
M06	0.05	0.09	0.05	0.12	0.22	0.23	**0.13**
M06-2X	0.04	0.01	0.05	0.02	0.15	0.11	**0.06**
M06-HF	0.35	0.32	0.36	0.31	0.13	0.16	**0.27**
PBE	0.17	0.14	0.02	0.14	0.16	0.16	**0.13**
PW91	0.16	0.12	0.01	0.15	0.17	0.17	**0.13**
ωB97X	0.17	0.15	0.21	0.10	0.04	0.05	**0.12**
ωB97X-D	0.12	0.09	0.22	0.14	0.07	0.06	**0.12**
mean	**0.15**	**0.15**	**0.12**	**0.17**	**0.18**	**0.17**	**0.15**

the most reliable functionals when averaged over all basis sets considered.

Accurately modeling the barrier separating the *syn* and *anti* conformers is vital for reliable simulations of the behavior of conjugated organic oligomers. Unfortunately, errors in predicted torsional barriers for the DFT functionals tested were considerably larger than those observed for the relative conformational energies. These errors are provided in Table 4. Errors in predicted dihedral angles are available in SI Table S3. Again, empirical dispersion corrections provide little improvement in predicted torsional barrier heights and actually lead to larger errors in many cases. This is particularly true in the case of B3LYP-D. Considering the M06 family of functionals, we again see a complicated dependence on the amount of HF exchange. In particular, M06-HF provides the most accurate torsional barriers for bifuran, while M06-2X shines for bithiophene and biselenophene.

Although all of the levels of theory tested predict transition states with dihedral angles within 5° of the FPA value for bifuran, few of these levels of theory provide torsional barriers within 0.1 kcal mol^{-1} of the benchmark value. Moreover, some levels of theory, mainly those utilizing cc-pVDZ and the GGA and hybrid DFT functionals, provide barriers deviating from the benchmark value by almost 2 kcal mol^{-1}. Overall, the M06-HF, ωB97X, and ωB97X-D functionals as well as the Pople-style basis sets generally provided the most reliable torsional barriers for bifuran.

The dihedral angle for the *syn-anti* transition state for bithiophene is even better geometrically described by these DFT functionals than bifuran. In fact, the dihedral angle for all predicted torsional transition states are within 1° of the FPA

dx.doi.org/10.1021/ct5004725 | J. Chem. Theory Comput. 2014, 10, 3647−3655

Table 4. Errors in Predicted Torsional Barriers (kcal mol^{-1}), Relative to the *anti* Conformer, When Compared to the FPA Benchmarks

	6-31+G(d)	6-31++G(d)	6-311++G(d)	cc-pVDZ	aug-cc-pVTZ	TZVPP	**mean**
			Bifuran				
B2PLYP	0.28	0.27	0.20	0.96	0.39	0.39	**0.42**
B2PLYP-D	0.11	0.10	0.03	1.13	0.58	0.56	**0.42**
B3LYP	0.81	0.81	0.78	1.78	1.05	1.07	**1.05**
B3LYP-D	1.14	1.14	1.10	2.11	1.38	1.40	**1.38**
B97-D	0.99	0.97	0.95	1.90	1.32	1.33	**1.25**
M06	1.76	1.77	1.59	2.45	1.98	2.04	**1.93**
M06-2X	0.69	0.70	0.71	1.43	1.07	0.97	**0.93**
M06-HF	0.08	0.08	0.02	0.54	0.30	0.10	**0.19**
PBE	0.73	0.71	0.68	1.70	1.07	1.07	**0.99**
PW91	0.80	0.78	0.74	1.78	1.12	1.12	**1.06**
ωB97X	0.24	0.24	0.25	0.54	0.01	0.01	**0.21**
ωB97X-D	0.02	0.01	0.07	0.76	0.22	0.22	**0.21**
mean	**0.64**	**0.63**	**0.59**	**1.42**	**0.87**	**0.86**	**0.84**
			Bithiophene				
B2PLYP	0.63	0.57	0.48	0.07	0.18	0.06	**0.33**
B2PLYP-D	0.45	0.39	0.30	0.28	0.38	0.26	**0.34**
B3LYP	0.00	0.02	0.05	0.48	0.38	0.29	**0.20**
B3LYP-D	0.40	0.41	0.32	0.90	0.78	0.68	**0.58**
B97-D	0.58	0.59	0.49	1.18	0.88	0.81	**0.75**
M06	0.63	0.68	0.64	0.96	1.36	1.29	**0.93**
M06-2X	0.09	0.07	0.04	0.30	0.56	0.41	**0.25**
M06-HF	1.05	1.04	0.97	0.58	0.51	0.56	**0.79**
PBE	0.40	0.42	0.32	1.03	0.78	0.69	**0.61**
PW91	0.43	0.44	0.34	1.10	0.81	0.73	**0.64**
ωB97X	0.63	0.61	0.57	0.16	0.15	0.25	**0.40**
ωB97X-D	0.68	0.66	0.65	0.32	0.26	0.35	**0.49**
mean	**0.50**	**0.49**	**0.43**	**0.61**	**0.59**	**0.53**	**0.53**
			Biselenophene				
B2PLYP	0.02	0.04	0.46	0.08	0.09	0.02	**0.12**
B2PLYP-D	0.24	0.22	0.21	0.17	0.35	0.28	**0.24**
B3LYP	0.27	0.23	0.26	0.14	0.13	0.10	**0.19**
B3LYP-D	0.79	0.75	0.26	0.66	0.63	0.61	**0.62**
B97-D	0.94	0.90	0.40	0.91	0.76	0.78	**0.78**
M06	0.87	0.85	0.49	0.60	1.01	1.04	**0.81**
M06-2X	0.35	0.33	0.05	0.04	0.42	0.34	**0.25**
M06-HF	0.60	0.63	1.05	0.83	0.53	0.62	**0.71**
PBE	0.70	0.66	0.15	0.63	0.57	0.57	**0.55**
PW91	0.72	0.68	0.17	0.68	0.61	0.62	**0.58**
ωB97X	0.31	0.34	0.78	0.50	0.46	0.49	**0.48**
ωB97X-D	0.48	0.50	0.92	0.70	0.60	0.62	**0.63**
mean	**0.52**	**0.51**	**0.43**	**0.50**	**0.51**	**0.51**	**0.50**

value. Overall, the M06-2X and B3LYP functionals, when paired with the three Pople basis sets, are among the top eight performing levels of theory. Satisfyingly, none of the methods tested provide barriers that deviate from the benchmark by more than 1.2 kcal mol^{-1}. Overall, though, the Pople-style basis sets provide slightly more reliable energetic barriers than the other basis sets. Averaging over all of the basis sets considered, the B3LYP and M06-2X functionals offer the most reliable barriers for bithiophene, although many functional/basis set combinations provide reliable predictions.

The methods tested also provide accurate torsional barriers for biselenophene, with all of the methods predicting barriers within 2° of the FPA value. The better performing levels of theory include B2PLYP paired with a variety of basis sets as well as M06-2X with either 6-311++G(d) or cc-pVDZ. Overall, the 6-311++G(d) basis set leads to the most reliable torsional barriers for biselenophene. Additionally, averaged across all basis sets, the best performing functionals are B2PLYP and B3LYP.

IV. SUMMARY AND CONCLUDING REMARKS

We have provided highly accurate gas-phase torsional potentials for bifuran, bithiophene, and biselenophene using focal point analyses. Bifuran has a very small energy maximum at the fully planar *syn* geometry, indicating similarity with bithiophene and biselenophene. However, the width of the wells containing the minima will be the main contributing factor to the nonplanarity and torsional flexibility of these systems. Overall, MP2, when paired with sufficiently large basis sets, provides robust predictions of the torsional potentials of these systems, justifying its use in the parametrization of MM force fields.

We have made further comparison of these potentials to those derived using various DFT functionals and basis sets. First, we found that the BC6-31G basis set for selenium reported by Binning and Curtiss[88] produces highly irregular and inaccurate potentials for biselenophene and should be avoided. The newer 6-31G basis set, from Rossalov and co-workers,[42] provides much more realistic potentials. Overall, we found that modern DFT functionals provide remarkably accurate relative energies for the *syn* and *anti* conformers, and many modern DFT functionals yield highly accurate torsional barriers for these model building blocks for conjugated oligomers. Among the better performers are ωB97X, B2PLYP, and B2PLYP-D with either the TZVPP or aug-cc-pVTZ basis sets as well as M06-2X/6-311++G(d). Surprisingly, the empirical dispersion correction of Grimme[59] leads to larger errors in both relative conformational energies and torsional barriers for these systems. Also, in contrast to the observations of Brédas and co-workers[41] for polyacetylene and polydiacetylene, we find no clear trend with regard to the impact of the amount of HF exchange for the M06 family of functionals. In particular, whereas the additional HF exchange of the M06-HF functional does provide enhanced performance for the torsional barrier for bifuran, M06-2X is the more reliable functional for the torsional barriers of bithiophene and biselenophene.

The identification of DFT functionals that provide reliable predictions of the torsional potentials of bifuran, bithiophene, and biselenophene should enable more reliable computational studies of oligomers and polymers comprising these building blocks. However, we note that the excellent performance of these functionals for the model systems examined does not guarantee their continued performance for larger oligomers. Indeed, many DFT functionals struggle to adequately predict properties of extended conjugated chains due, among other issues, to many-electron self-interaction error.[41,93,94] Regardless, the present benchmarks provide a starting point for the assessment of the performance of DFT methods and for more robust parametrizations of the torsional components of molecular mechanical force fields for oligofurans, oligothiophenes, and oligoselenophenes.

■ ASSOCIATED CONTENT

Supporting Information

Optimized geometries, additional data. This material is available free of charge via the Internet at http://pubs.acs.org.

■ AUTHOR INFORMATION

Corresponding Author

*E-mail: wheeler@chem.tamu.edu.

Notes

The authors declare no competing financial interest.

■ ACKNOWLEDGMENTS

This work was supported in part by the ACS Petroleum Research Fund (ACS PRF 50645-DNI6). We also thank the Texas A&M Supercomputing facility for providing computational resources.

■ REFERENCES

(1) Coropceanu, V.; Cornil, J.; da Silva Filho, D. A.; Olivier, Y.; Silbey, R.; Brédas, J.-L. *Chem. Rev.* **2007**, *107*, 926−952.
(2) Brédas, J.-L.; Norton, J. E.; Cornil, J.; Coropceanu, V. *Acc. Chem. Res.* **2009**, *42*, 1691−1699.
(3) Zade, S. S.; Bendikov, M. *Chem.—Eur. J.* **2007**, *13*, 3688−3700.
(4) Patra, A.; Bendikov, M. *J. Mater. Chem.* **2010**, *20*, 422.
(5) Bunz, U. H. F. *Angew. Chem., Int. Ed.* **2010**, *49*, 5037−5040.
(6) Gidron, O.; Varsano, N.; Shimon, L. J. W.; Leitus, G.; Bendikov, M. *Chem. Commun. (Cambridge, U. K.)* **2013**, *49*, 6256−6258.
(7) Bunz, U. H. F. *Angew. Chem., Int. Ed.* **2010**, *49*, 5037−5040.
(8) Zade, S. S.; Bendikov, M. *Chem.—Eur. J.* **2008**, *14*, 6734−6741.
(9) van Eijck, L.; Johnson, M. R.; Kearley, G. J. *J. Phys. Chem. A* **2003**, *107*, 8980−8984.
(10) Takayanagi, M.; Gejo, T.; Hanazaki, I. *J. Phys. Chem.* **1994**, *98*, 12893−12898.
(11) Fabiano, E.; Della Sala, F. *Chem. Phys. Lett.* **2006**, *418*, 496−501.
(12) Duarte, H. A.; Dos Santos, H. F.; Rocha, W. R.; De Almeida, W. B. *J. Chem. Phys.* **2000**, *113*, 4206.
(13) Raos, G. *Chem. Phys. Lett.* **2003**, *379*, 364−372.
(14) Bjorgaard, J. A.; Köse, M. E. *J. Phys. Chem. A* **2013**, *117*, 3869−3876.
(15) Guo, X.; Quinn, J.; Chen, Z.; Usta, H.; Zheng, Y.; Xia, Y.; Hennek, J. W.; Ortiz, R. P.; Marks, T. J.; Facchetti, A. *J. Am. Chem. Soc.* **2013**, *135*, 1986−1996.
(16) Jackson, N. E.; Savoie, B. M.; Kohlstedt, K. L.; Olvera de la Cruz, M.; Schatz, G. C.; Chen, L. X.; Ratner, M. A. *J. Am. Chem. Soc.* **2013**, *135*, 10475−10483.
(17) Samdal, S.; Samuelsen, E. J.; Volden, H. V. *Synth. Met.* **1993**, *59*, 259−265.
(18) Fedor, A. M.; Allis, D. G.; Korter, T. M. *Vib. Spectrosc.* **2009**, *49*, 124−132.
(19) Chaloner, P. A.; Gunatunga, S. R.; Hitchcock, P. B. *Acta Crystallogr., Sect. C* **1994**, *50*, 1941−1942.
(20) Pelletier, M.; Brisse, F. *Acta Crystallogr., Sect. C* **1994**, *50*, 1942−1945.
(21) Vujanovich, E. C.; Bloom, J. W. G.; Wheeler, S. E. *J. Phys. Chem. A* **2012**, *116*, 2997−3003.
(22) Gidron, O.; Diskin-Posner, Y.; Bendikov, M. *J. Am. Chem. Soc.* **2010**, *132*, 2148−2150.
(23) Duarte, H. A.; Duani, H.; De Almeida, W. B. *Chem. Phys. Lett.* **2003**, *369*, 114−124.
(24) Karpfen, A.; Choi, C. H.; Kertesz, M. *J. Phys. Chem. A* **1997**, *101*, 7426−7433.
(25) Orti, E.; Sanchez-Marin, J.; Merchan, M.; Tomas, F. *J. Phys. Chem.* **1987**, *91*, 545−551.
(26) Balbás, A.; González Tejera, M. J.; Tortajada, J. *J. Mol. Struct.: THEOCHEM* **2001**, *572*, 141−150.
(27) Liu, F.; Zuo, P.; Meng, L.; Zheng, S. *J. Mol. Struct.: THEOCHEM* **2005**, *726*, 189−196.
(28) Sancho-García, J. C.; Karpfen, A. *Theor. Chem. Acc.* **2006**, *115*, 427−433.
(29) Salzner, U.; Aydin, A. *J. Chem. Theory Comput.* **2011**, *7*, 2568−2583.
(30) Chidichimo, G.; Lelj, F.; Longeri, M.; Russo, N.; Veracini, C. A. *Chem. Phys. Lett.* **1979**, *67*, 384−387.
(31) Lee, S. K.; Cho, N. S.; Cho, S.; Moon, S.-J.; Lee, J. K.; Bazan, G. C. *J. Polym. Sci., Part A: Polym. Chem.* **2009**, *47*, 6873−6882.
(32) Lee, W.-H.; Lee, S. K.; Son, S. K.; Choi, J.-E.; Shin, W. S.; Kim, K.; Lee, S.-H.; Moon, S.-J.; Kang, I.-N. *J. Polym. Sci., Part A: Polym. Chem.* **2012**, *50*, 551−561.
(33) Lin, H.-W.; Lee, W.-Y.; Lu, C.; Lin, C.-J.; Wu, H.-C.; Lin, Y.-W.; Ahn, B.; Rho, Y.; Ree, M.; Chen, W.-C. *Polym. Chem.* **2012**, *3*, 767−777.
(34) Millefiori, S.; Alparone, A. *Synth. Met.* **1998**, *95*, 217−224.
(35) Sánchez-Sanz, G.; Alkorta, I.; Elguero, J. *Comput. Theor. Chem.* **2011**, *974*, 37−42.
(36) Gus'kova, O. A.; Khalatur, P. G.; Khokhlov, A. R. *Macromol. Theory Simul.* **2009**, *18*, 219−246.
(37) Marcon, V.; Raos, G. *J. Phys. Chem. B* **2004**, *108*, 18053−18064.
(38) DuBay, K. H.; Hall, M. L.; Hughes, T. F.; Wu, C.; Reichman, D. R.; Friesner, R. A. *J. Chem. Theory Comput.* **2012**, *8*, 4556−4569.
(39) Dahlgren, M. K.; Schyman, P.; Tirado-Rives, J.; Jorgensen, W. L. *J. Chem. Inf. Model.* **2013**, *53*, 1191−1199.

(40) Huang, J.-D.; Wen, S.-H.; Deng, W.-Q.; Han, K.-L. *J. Phys. Chem. B* **2011**, *115*, 2140−2147.
(41) Sutton, C.; Körzdörfer, T.; Gray, M. T.; Brunsfeld, M.; Parrish, R. M.; Sherrill, C. D.; Sears, J. M.; Brédas, J.-L. *J. Chem. Phys.* **2014**, 140.
(42) Allen, W. D.; East, A. L. L.; Császár, A. G. In *Structures and Conformations of Non-Rigid Molecules*; Laane, J., Dakkouri, M., van der Veken, B., Oberhammer, H., Eds.; Kluwer: Dordrecht, 1993; pp 343−373.
(43) Császár, A. G.; Allen, W. D.; Schaefer, H. F. *J. Chem. Phys.* **1998**, *108*, 9751−9764.
(44) East, A. L. L.; Allen, W. D. *J. Chem. Phys.* **1993**, *99*, 4638−4650.
(45) Schuurman, M. S.; Muir, S. R.; Allen, W. D.; Schaefer, H. F. *J. Chem. Phys.* **2004**, *120*, 11586−11599.
(46) Dunning, T. H., Jr. *J. Chem. Phys.* **1989**, *90*, 1007−1023.
(47) Woon, D. E.; Dunning, J. T. H. *J. Chem. Phys.* **1993**, *98*, 1358−1371.
(48) Wilson, A. K.; Woon, D. E.; Peterson, K. A.; Dunning, J. T. H. *J. Chem. Phys.* **1999**, *110*, 7667−7676.
(49) Feller, D. *J. Chem. Phys.* **1993**, *98*, 7059−7071.
(50) Helgaker, T.; Klopper, W.; Koch, H.; Noga, J. *J. Chem. Phys.* **1997**, *106*, 9639−9646.
(51) MOLPRO, version 2010.1, is a package of ab initio programs written by H.-J. Werner et al.
(52) CFOUR, Coupled-Cluster techniques for Computational Chemistry, a quantum-chemical program package by Stanton, J. F.; Gauss, J.; Harding, M. E.; Szalay, P. G. with contributions from Auer, A. A.; Bartlett, R. J.; Benedikt, U.; Berger, C.; Bernholdt, D. E.; Bomble, Y. J.; Cheng, L.; Christiansen, O.; Heckert, M.; Heun, O.; Huber, C.; Jagau, T.-C.; Jonsson, D.; Jusélius, J.; Klein, K.; Lauderdale, W. J.; Matthews, D. A.; Metzroth, T.; Mück, L. A.; O'Neill, D. P.; Price, D. R.; Prochnow, E.; Puzzarini, C.; Ruud, K.; Schiffmann, F.; Schwalbach, W.; Simmons, C.; Stopkowicz, S.; Tajti, A.; Vázquez, J.; Wang, F.; Watts, J. D. and the integral packages MOLECULE (Almlöf, J.; Taylor, P. R.), PROPS (Taylor, P. R.), and ABACUS (Helgaker, T.; Jensen, H. J. Aa.; Jørgensen, P.; Olsen, J.) and ECP routines by Mitin, A. V.; van Wüllen, C.
(53) Grimme, S. *J. Chem. Phys.* **2006**, *124*, 034108−034116.
(54) Schwabe, T.; Grimme, S. *Phys. Chem. Chem. Phys.* **2007**, *9*, 3397−3406.
(55) Becke, A. D. *J. Chem. Phys.* **1993**, *98*, 5648−5652.
(56) Lee, C.; Yang, W.; Parr, R. G. *Phys. Rev. B* **1988**, *37*, 785−789.
(57) Stephens, P. J.; Devlin, F. J.; Chabalowski, C. F.; Frisch, M. J. *J. Phys. Chem.* **1994**, *98*, 11623−11627.
(58) Vosko, S. H.; Wilk, L.; Nusair, M. *Can. J. Phys.* **1980**, *58*, 1200−1211.
(59) Grimme, S. *J. Comput. Chem.* **2006**, *27*, 1787−1799.
(60) Becke, A. *J. Chem. Phys.* **1997**, *107*, 8554−8560.
(61) Zhao, Y.; Truhlar, D. *Theor. Chem. Acc.* **2008**, *120*, 215−241.
(62) Perdew, J. P.; Burke, K.; Ernzerhof, M. *Phys. Rev. Lett.* **1996**, *77*, 3865−3868.
(63) Perdew, J. P.; Burke, K.; Ernzerhof, M. *Phys. Rev. Lett.* **1997**, *78*, 1396−1396.
(64) Perdew, J. P.; Burke, K.; Wang, Y. *Phys. Rev. B* **1996**, *54*, 16533−16539.
(65) Perdew, J. P.; Chevary, J. A.; Vosko, S. H.; Jackson, K. A.; Pederson, M. R.; Singh, D. J.; Fiolhais, C. *Phys. Rev. B* **1993**, *48*, 4978−4978.
(66) Perdew, J. P.; Chevary, J. A.; Vosko, S. H.; Jackson, K. A.; Pederson, M. R.; Singh, D. J.; Fiolhais, C. *Phys. Rev. B* **1992**, *46*, 6671−6687.
(67) Chai, J.-D.; Head-Gordon, M. *J. Chem. Phys.* **2008**, *128*, 084106−084115.
(68) Chai, J.-D.; Head-Gordon, M. *Phys. Chem. Chem. Phys.* **2008**, *10*, 6615−6620.
(69) Hehre, W. J.; Ditchfield, R.; Pople, J. A. *J. Chem. Phys.* **1972**, *56*, 2257−2261.
(70) Francl, M. M.; Pietro, W. J.; Hehre, W. J.; Binkley, J. S.; Gordon, M. S.; DeFrees, D. J.; Pople, J. A. *J. Chem. Phys.* **1982**, *77*, 3654−3665.
(71) Clark, T.; Chandrasekhar, J.; Spitznagel, G. W.; Schleyer, P. v. R. *J. Comput. Chem.* **1983**, *4*, 294−301.
(72) Hariharan, P. C.; Pople, J. A. *Theor. Chim. Acta* **1973**, *28*, 213−222.
(73) Frisch, M. J.; Pople, J. A.; Binkley, J. S. *J. Chem. Phys.* **1984**, *80*, 3265−3269.
(74) McLean, A. D.; Chandler, G. S. *J. Chem. Phys.* **1980**, *72*, 5639−5648.
(75) Curtiss, L. A.; McGrath, M. P.; Blaudeau, J.-P.; Davis, N. E.; Binning, J. R. C.; Radom, L. *J. Chem. Phys.* **1995**, *103*, 6104−6113.
(76) Davidson, E. R. *Chem. Phys. Lett.* **1996**, *260*, 514−518.
(77) Kendall, R. A.; Dunning, T. H., Jr.; Harrison, R. J. *J. Chem. Phys.* **1992**, *96*, 6796−6806.
(78) Feller, D. *J. Comput. Chem.* **1996**, *17*, 1571−1586.
(79) Weigend, F.; Ahlrichs, R. *Phys. Chem. Chem. Phys.* **2005**, *7*, 3297−3305.
(80) Schuchardt, K. L.; Didier, B. T.; Elsethagen, T.; Sun, L.; Gurumoorthi, V.; Chase, J.; Li, J.; Windus, T. L. *J. Chem. Inf. Model.* **2007**, *47*, 1045−1052.
(81) Gräfenstein, J.; Cremer, D. *J. Chem. Phys.* **2007**, *127*, 164113.
(82) Gräfenstein, J.; Izotov, D.; Cremer, D. *J. Chem. Phys.* **2007**, *127*, 214103.
(83) Johnson, E. R.; Becke, A. D.; Sherrill, C. D.; DiLabio, G. A. *J. Chem. Phys.* **2009**, *131*, 034111.
(84) Wheeler, S. E.; Houk, K. N. *J. Chem. Theory Comput.* **2010**, *6*, 395−404.
(85) Frisch, M. J.; Trucks, G. W.; Schlegel, H. B.; Scuseria, G. E.; Robb, M. A.; Cheeseman, J. R.; Scalmani, G.; Barone, V.; Mennucci, B.; Petersson, G. A.; Nakatsuji, H.; Caricato, M.; Li, X.; Hratchian, H. P.; Izmaylov, A. F.; Bloino, J.; Zheng, G.; Sonnenberg, J. L.; Hada, M.; Ehara, M.; Toyota, K.; Fukuda, R.; Hasegawa, J.; Ishida, M.; Nakajima, T.; Honda, Y.; Kitao, O.; Nakai, H.; Vreven, T.; Montgomery, J. A., Jr.; Peralta, J. E.; Ogliaro, F.; Bearpark, M.; Heyd, J. J.; Brothers, E.; Kudin, K. N.; Staroverov, V. N.; Kobayashi, R.; Normand, J.; Raghavachari, K.; Rendell, A.; Burant, J. C.; Iyengar, S. S.; Tomasi, J.; Cossi, M.; Rega, N.; Millam, N. J.; Klene, M.; Knox, J. E.; Cross, J. B.; Bakken, V.; Adamo, C.; Jaramillo, J.; Gomperts, R.; Stratmann, R. E.; Yazyev, O.; Austin, A. J.; Cammi, R.; Pomelli, C.; Ochterski, J. W.; Martin, R. L.; Morokuma, K.; Zakrzewski, V. G.; Voth, G. A.; Salvador, P.; Dannenberg, J. J.; Dapprich, S.; Daniels, A. D.; Farkas, Ö.; Foresman, J. B.; Ortiz, J. V.; Cioslowski, J.; Fox, D. J. *Gaussian 09, Revision B.01*; Gaussian, Inc.: Wallingford, CT, 2009.
(86) Mitin, A. V. *J. Comput. Chem.* **2013**, *34*, 2014−2019.
(87) Mitin, A. V.; Merz, K. M. *Int. J. Quantum Chem.* **2007**, *107*, 3028−3038.
(88) Binning, R. C.; Curtiss, L. A. *J. Comput. Chem.* **1990**, *11*, 1206−1216.
(89) Rassolov, V. A.; Ratner, M. A.; Pople, J. A.; Redfern, P. C.; Curtiss, L. A. *J. Comput. Chem.* **2001**, *22*, 976−984.
(90) Mitin, A. V.; Baker, J.; Pulay, P. *J. Chem. Phys.* **2003**, *118*, 7775−7782.
(91) Islam, S. M.; Poirier, R. A. *J. Phys. Chem. A* **2007**, *111*, 13218−13232.
(92) Islam, S. M.; Huelin, S. D.; Dawe, M.; Poirier, R. A. *J. Chem. Theory Comput.* **2007**, *4*, 86−100.
(93) Körzdörfer, T.; Parrish, R. M.; Sears, J. M.; Sherrill, C. D.; Brédas, J.-L. *J. Chem. Phys.* **2012**, *137*, 124305.
(94) Körzdörfer, T.; Sears, J. M.; Sutton, C.; Brédas, J.-L. *J. Chem. Phys.* **2011**, 135.